Using optical clock transitions in Cu II and Yb III for timekeeping and search for new physics

Saleh O. Allehabi,[1] V. A. Dzuba,[1] and V. V. Flambaum[1,2]
[1]*School of Physics, University of New South Wales, Sydney 2052, Australia*
[2]*Helmholtz Institute Mainz, Johannes Gutenberg University, 55099 Mainz, Germany*

(Received 13 September 2021; accepted 1 November 2021; published 17 November 2021)

We study the $^1S_0 - {}^3D_2$ and $^1S_0 - {}^3D_3$ transitions in Cu II and the $^1S_0 - {}^3P^o_2$ transition in Yb III as possible candidates for the optical clock transitions. A recently developed version of the configuration interaction method, designed for a large number of electrons above the closed-shell core, is used to carry out the calculation. We calculate excitation energies, transition rates, lifetimes, and scalar static polarizabilities of the ground, clock states, and blackbody radiation shift. We demonstrate that the considered transitions have all features of the clock transition leading to prospects of highly accurate measurements. A search for new physics, such as time variation of the fine-structure constant, is also investigated.

DOI: 10.1103/PhysRevA.104.053109

I. INTRODUCTION

Extremely high accuracy of the frequency measurements for the optical clock transitions naturally lead to the use of the transitions not only for time keeping, but also for the search of the manifestations of new physics beyond the standard model, such as local Lorentz invariance (LLI) violation and time variation of the fine-structure constant ($\alpha = e^2/\hbar c$) (see, e.g., Refs. [1–8]). Oscillating variation of the fine-structure constant may be produced by interaction of a low-mass scalar dark matter field with a photon field (see, e.g., Refs. [9–13]). Therefore, the measurement of such variation provides an efficient method to search for dark matter using atomic clocks, which have already provided improvement of the constraints on the scalar-photon interaction constants up to 15 orders of magnitude [9–13].

The search for new physics with atomic clocks usually involves measuring the frequencies of two clock transitions against each other over a long period of time. Both transitions must be very narrow and not sensitive to perturbation to allow extremely high accuracy of the measurements. They also must have different sensitivities to new physics so that under the studied effect, frequencies change at different rates and maybe even in different directions. Having both transitions in the same atom brings additional convenience.

The relative uncertainty of the frequency measurements for the best optical clocks is on the level of 10^{-18}. For example, it is 9.4×10^{-19} for Al^+ [4], 3.0×10^{-18} for Yb^+ [6], and 1×10^{-18} for Yb [14]. Unfortunately, most of working optical clocks are not very sensitive to new physics. Among the examples listed above, only Yb^+ clock transition is highly sensitive to a variation of the fine-structure constant [2,15,16] and to the LLI violation [3,17]. Therefore, there is an ongoing search for new clock transitions which may combine high accuracy of the measurements with high sensitivity to new physics, e.g., to the time variation of the fine-structure constant. One way of achieving this is to use highly charged ions [18]. This is now a large area of research with very promising perspectives (see, e.g., Refs. [19–21]).

Neutral or nearly neutral atoms are also considered. The important advantage of using them is that they are very well studied. In some cases, new promising transitions can be found in atoms that are already used for a high accuracy atomic clock. E.g., new transitions in Yb were recently suggested [22,23] in addition to the currently used $^1S_0 - {}^3P^o_0$ clock transition. Clock transitions between metastable states in Yb II have been suggested in Ref. [24]. A good guide for finding atomic clock transitions sensitive to variations of α is to look for metastable states which are connected to the ground state (GS) via transitions that can be approximately considered as $s - d$, $s - f$, or $p - f$ single-electron transitions [25]. The $s - d$ transitions of this kind were considered in Cu, Ag, and Au atoms in Ref. [26].

In the present paper, we consider the $^1S_0 - {}^3D_2$ and $^1S_0 - {}^3D_3$ transitions in Cu II and the $^1S_0 - {}^3P^o_2$ transition in Yb III (see Figs. 1 and 2). Transitions in Cu II are the $s - d$ transitions, the transition in Yb III is the $s - f$ transition. In our early work [15], we suggested to use the $4f^{14}\ {}^1S_0 - 4f^{13}5d\ {}^3P^o_0$ in Yb III for the search of the variation of the fine-structure constant. The prospect for precision measurement of the frequency of this transition was considered in a recent paper [27]. However, this transition has an important drawback. There is a decay channel via magnetic dipole transition ($M1$) into the lower-lying state $4f^{13}5d\ {}^3P^o_1$. This may make the considered transition not be sufficiently narrow to ensure high accuracy of the measurements. This problem was not discussed in Refs. [15] or [27]. In the present paper, we consider a different transition, a transition from the ground state to the first excited-state $4f^{13}5d\ {}^3P^o_2$.

This is a very narrow transition with a similar sensitivity to the variation of the fine-structure constant. We demonstrate that it has all features of the atomic clock transition.

Several studies have analyzed the energies and transition probabilities for both ions, Cu II [28–30] and Yb III [31,32]

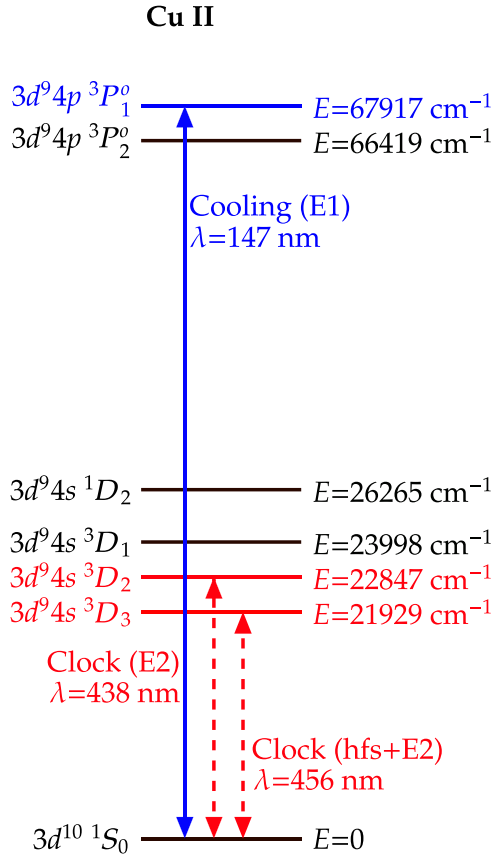

FIG. 1. The energy diagram for the states of the Cu II ion relevant for the optical ion clock. The electric dipole cooling transition is shown as a solid blue line, and the clock transitions are shown as short-dashed red lines.

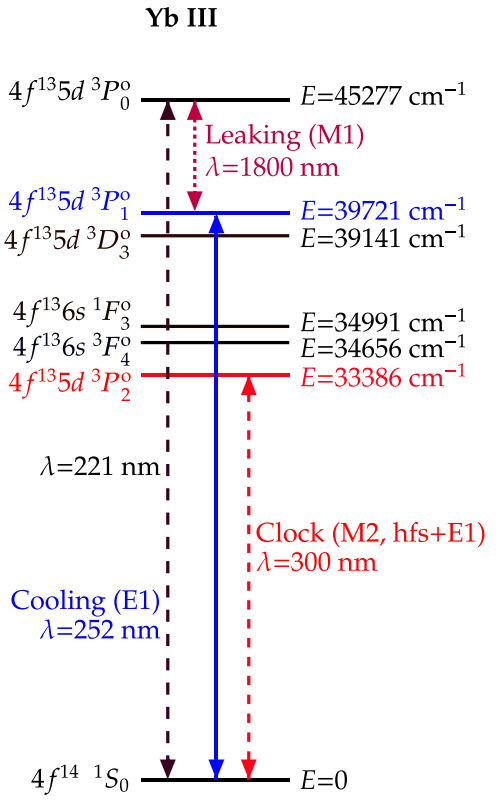

FIG. 2. The energy diagram for the states of the Yb III ion relevant for the optical ion clock. The electric dipole cooling transition is shown as a solid blue line, the clock transition is shown as a short-dashed red line, and the purple dotted lines show the leakage transition.

theoretically and experimentally (see also Ref. [33] and references therein). This gives us an opportunity to compare results to have confidence in the accuracy of the analysis. None of the previous studies focused on transitions in Cu II and Yb III in sufficient detail to study their suitability for time keeping and searching for new physics.

II. METHOD OF CALCULATION

As can be seen from the spectra of the Cu II and Yb III ions, the excited states of the Cu II ion have an open $3d$ shell, and the excited states of the Yb III ion have an open $4f$ shell. Therefore, to perform the electron structure calculations for both ions, the recent version of the configuration interaction (CI) method was used, which has been designed to deal with a large number of valence electrons [34]. The method combines CI with perturbation theory (PT) and is called the CIPT method. The method reduces the size of the effective CI matrix by neglecting the off-diagonal matrix elements between high-energy basis states and reducing their contribution to PT corrections to the matrix elements between low-energy basis states.

The eigenvalues E and eigenstates ψ can be found by solving the CI equations with the effective $H^{\rm CI}$ matrix,

$$(H^{\rm CI} - EI)\psi = 0, \tag{1}$$

where I is the unit matrix. Matrix elements of the effective CI matrix contain PT-type corrections from the high-energy states,

$$\langle a|H^{\rm CI}|b\rangle \to \langle a|H^{\rm CI}|b\rangle + \sum_h \frac{\langle a|H^{\rm CI}|h\rangle\langle h|H^{\rm CI}|b\rangle}{E - E_h}. \tag{2}$$

Here a and b are low-energy states, and E_h is the diagonal matrix element between high-energy states ($E_h = \langle h|H^{\rm CI}|h\rangle$).

To produce a set of complete single-electron basis states for both ions, we start the calculations with the Dirac-Hartree-Fock (DHF) method in the V^N approximation with all atomic electrons included. It seems to be natural to start from the [Ar]$3d^{10}$ configuration for Cu II and the [Xe]$4f^{14}$ configuration for Yb III. However, such a choice of initial approximation is good for calculating the ground states of the ions. Since we need to calculate excited states as well, which have excitations from the $3d$ or $4f$ subshell, the choice of initial approximation is not obvious, and it is dictated by the accuracy of the final results. It turns out that the best results are obtained if we start from the [Ar]$3d^9 4s$ configuration for Cu II and the [Xe]$4f^{14}$ configuration for Yb III.

The single-electron basis states are then constructed using B splines [35,36] with 40 B-spline states on the order of $k = 9$ in a box of the radius $R_{\rm max} = 40a_B$ with orbital angular momentum $0 \leqslant l \leqslant 4$.

To carry out the calculations of the transition amplitudes and hyperfine structure (hfs), we use the time-dependent HF method [37], which is equivalent to the random-phase approximation (RPA). The RPA equations can be written as

$$(\hat{H}^{\rm RHF} - \epsilon_c)\delta\psi_c = -(\hat{d} + \delta V^N)\psi_c. \tag{3}$$

Here, the relativistic Hartree-Fock is (RHF), $\hat{d}$ refers to the operator of an external field, which can be any field, which is sufficiently weak to be considered in linear approximation. ϵ_c is the energy of electron state c, ψ_c is the state wave function, and δV^N denotes the correction to the self-consistent potential caused by the effect of an external field. Equation (3) is solved self-consistently for all states c in the core. As a result, the correction to the core potential δV^N is found. Then reduced matrix elements for valence states are calculated using the expression,

$$A_{b\to a} \equiv \langle\psi_a||\hat{d} + \delta V^N||\psi_b\rangle. \tag{4}$$

The electric dipole ($E1$), magnetic dipole ($M1$), electric quadrupole ($E2$), magnetic quadrupole ($M2$), and electric octupole ($E3$) transition probabilities (in atomic units) from upper state b to lower state a can be written as

$$T_{E1,M1} = \frac{4}{3}(\alpha\omega)^3\frac{A^2_{E1,M1}}{2J_b+1}, \tag{5}$$

$$T_{E2,M2} = \frac{1}{15}(\alpha\omega)^5\frac{A^2_{E2,M2}}{2J_b+1}, \tag{6}$$

$$T_{E3} = 0.001\,69(\alpha\omega)^7\frac{A^2_{E3}}{2J_b+1}. \tag{7}$$

Here α is the fine-structure constant, ω is the energy difference between the lower and the upper states, A is the transition amplitude (4), J_b is the total angular momentum of the upper state b. Note that magnetic amplitudes $A_{M1,M2}$ contain the Bohr magneton μ_B ($\mu_B = \alpha/2 \approx 3.65\times10^{-3}$ in atomic units). For some strongly forbidden transitions leading contribution comes from electromagnetic transitions mediated by the hyperfine interaction. Clock transitions in ^{63,65}Cu II and ^{171,173}Yb III are good examples of such transitions. The transition amplitude is

$$A_{\text{hfs-}E1,E2}(b\to a) = \sum_n\left(\frac{\langle a|A_{\rm hfs}|n\rangle\langle n|A_{E1,E2}|b\rangle}{E_a - E_n} + \frac{\langle b|A_{\rm hfs}|n\rangle\langle n|A_{E1,E2}|a\rangle}{E_b - E_n}\right). \tag{8}$$

Here $A_{\rm hfs}$ is the operator of the magnetic dipole or electric quadrupole hfs interaction, $A_{E1,E2}$ are the operators of the $E1$ and $E2$ transitions. Summation in (8) goes over a complete set of intermediate states $|n\rangle$ (for more details, see, e.g., Refs. [29,38–40]). In practice, it is usually sufficient to include few close states into the summation over n. For example, the leading contribution to the transition amplitude of the $^1S_0 - {}^3D_3$ clock transition in Cu II comes from the electric quadrupole transition mediated by the magnetic dipole hfs interaction. It is sufficient to include three intermediate states into the summation, the $3d^9 4s\ {}^3D_2$, $^1D_2$, and $^3D_1$ states. Then Eq. (8) becomes

$$\begin{aligned} A_{\text{hfs-}E2}(3d^9 4s\,{}^3D_3 \to 3d^{10}\,{}^1S_0) &= \frac{\langle {}^3D_3|A_{\rm hfs}|{}^3D_2\rangle\langle {}^3D_2|A_{E2}|{}^1S_0\rangle}{E({}^3D_3) - E({}^3D_2)} \\ &+ \frac{\langle {}^3D_3|A_{\rm hfs}|{}^1D_2\rangle\langle {}^1D_2|A_{E2}|{}^1S_0\rangle}{E({}^3D_3) - E({}^1D_2)} \\ &+ \frac{\langle {}^3D_3|A_{E2}|{}^3D_1\rangle\langle {}^3D_1|A_{\rm hfs}|{}^1S_0\rangle}{E({}^1S_0) - E({}^3D_1)}. \end{aligned} \tag{9}$$

For the $^1S_0 - {}^3P^{\rm o}_2$ transition in the Yb III ion, the hyperfine-induced $E1$ transition amplitude is expressed as

$$\begin{aligned} A_{\text{hfs-}E1}(4f^{13}5d\,{}^3P^{\rm o}{}_2 \to 4f^{14}\,{}^1S_0) &= \frac{\langle {}^3P^{\rm o}{}_2|A_{\rm hfs}|{}^3P^{o}{}_1\rangle\langle {}^3P^{\rm o}{}_1|A_{E1}|{}^1S_0\rangle}{E\left({}^3P^{\rm o}_2\right) - E\left({}^3P^{\rm o}_1\right)}. \end{aligned} \tag{10}$$

Transition amplitudes (9) and (10) depend on the values of the total angular momentum F of a specific hfs state ($\mathbf{F} = \mathbf{J} + \mathbf{I}$, where $\mathbf{I}$ is the nuclear spin). Detailed equations can be found in Refs. [29,38–40]). To find corresponding transition rates, we use Eqs. (5) and (6), replacing A_{E1} by $A_{\text{hfs-}E1}$ in Eq. (5), and A_{E2} by $A_{\text{hfs-}E2}$ in Eq. (6).

Radiative lifetimes τ_b of each excited state b can be obtained as

$$\tau_b = 1\Big/\sum_a T_{ab}, \tag{11}$$

where the summation goes over all possible transitions to lower states a.

Accuracy of the calculations with the use of the CIPT method for complicated atomic systems (open p, d, and f shells) was studied in detail in our previous papers (see, e.g., Refs. [34,41–44]). It is about a few percent for the energies of low-lying states and about a few tens of percent for the matrix elements. Accuracy tends to go down for higher states due to proximity to the high-energy states, which are treated perturbatively. It is also lower for states of complicated configurations involving more than two single-electron states. This is due to a larger number of possibilities for exciting one or two electrons to different states leading to a very large basis of many-electron states. Only a small fraction of their states are included in the effective CI matrix [Eq. (2)], the rest are treated perturbatively. In principle, it is possible to improve the accuracy of calculations by moving the boundary between low- and high-energy states up the energy scale leading to the increased size of the effective CI matrix. However, it is a numerically expensive procedure, requiring large computer power. In the end, the accuracy of present calculations is sufficient for the purposes of present paper, which is checking that studied atomic systems can be used as atomic clocks.

III. RESULTS

A. Energy levels, transition probabilities, and lifetimes

Table I presents calculated energy levels and lifetimes of the low-energy states of Cu II and Yb III ions compared with experimental data and other calculations. The lifetimes were calculated using transition probabilities presented in

TABLE I. Excitation energies (E, cm^{-1}) and lifetimes (τ) for some low states of Cu II and Yb III ions.

			Energy (cm^{-1})			Lifetime		
				Other			Other	
No.	Conf.	Term	Present	NIST [33]	Cal.	Present	Expt.	Cal.
				Cu II				
1	$3d^{10}$	$^1S_0$	0	0	0	∞		
2	$3d^9 4s$	$^3D_3$	21932	21929	22469[a]	$\sim 10^8$ s		
3		$^3D_2$	22733	22847	23381[a]	7.8 s		
4		$^3D_1$	23705	23998	24495[a]			
5	$3d^9 4s$	$^1D_2$	25833	26265	26840[a]			
6	$3d^9 4p$	$^3P^o_2$	66623	66419	66984[b]			
7		$^3P^o_1$	67922	67917	68703[b]	2.2 ns	2.36 ± 0.05 ns[c]	2.39 ns, 2.21 ns[b]
				Yb III				
1	$4f^{14}$	$^1S_0$	0	0	0	∞		
2	$4f^{13}5d$	$(7/2, 3/2)^o_2 \equiv {}^3P^o_2$	29208	33386	39755[d]	$\sim$2000 s[e]		6017 s[d]
3	$4f^{13}5d$	$(7/2, 3/2)^o_3 \equiv {}^3D^o_3$	33839	39141	44429[d]			
4	$4f^{13}6s$	$(7/2, 1/2)^o_4 \equiv {}^3F^o_4$	35000	34656	36336[d]			
5	$4f^{13}6s$	$(7/2, 1/2)^o_3 \equiv {}^1F^o_3$	36418	34991	36764[d]			
6	$4f^{13}5d$	$(7/2, 5/2)^o_1 \equiv {}^3P^o_1$	35288	39721	39762[d]	250 ns	230(20) ns[f]	166 ns, 270 ns[f] 181 ns[d]
7	$4f^{13}5d$	$(5/2, 5/2)^o_0 \equiv {}^3P^o_0$	41059	45277	49469[d]	0.133 s		0.1490 s[d]

[a] Reference [29].
[b] Reference [30]; for the lifetime, the first value was obtained using the length gauge, and the second was obtained using the velocity gauge.
[c] Reference [28].
[d] Reference [31]; the value was obtained using the relativistic many-body perturbation theory (RMBPT) method.
[e] The $M2$ and hfs-$E1$ transitions are taken into account, see Tables II and III for details.
[f] Reference [32]; the first calculated value was obtained using the RHF method + core polarization (CP) effects, and the second calculated value was obtained using the same procedure with including $5s$, $5p$, and $4f$ to the CP effects.

Table II. The results for the energies are in sufficiently good agreement with experimental data from NIST. The average difference between the NIST and the calculated data for Cu II is $\sim 100\ \mathrm{cm}^{-1}$, whereas for Yb III, the difference is $\sim 4000\ \mathrm{cm}^{-1}$. Note that different sources present different state labeling for Yb III (see, e.g., Refs. [27,33]). Therefore, for the sake of easy comparison, we present in the table state labeling based on both commonly used schemes, the J-J and L-S schemes.

Table II presents calculated transition amplitudes and transition rates and compares them to the experimental data and other theoretical values. Lifetimes of the states calculated using transition rates from Table II are presented in Table I. As can be seen from the tables, the present results for the Cu II ion are in good agreement with the experimental data and other calculations. For the transition between the first excited-state $3d^9 4s\ ^3D_3$ and the ground state, the dominating contribution comes from the hfs-induced electric quadrupole transition [see Eq. (9)]. This transition was studied before in Ref. [29] using the same strategy. The results for two isotopes of Cu are compared in Table III, indicating good agreement. The same table shows hfs-induced transition rates for the clock state (c.s.) of ^{171}Yb and ^{173}Yb.

For the transition rates of the Yb III ion, we compared our results with the theoretical values of Safronova and Safronova [31]. They carried out theoretical calculations using the second-order RMBPT. The results are in reasonably good agreement with our calculations. The most noticeable disagreement is about two times difference in the $M2$ transition rate between the clock and the ground states. Given that hfs-induced $E1$ transition also gives a significant contribution to the transition rate, and this contribution was not considered in Ref. [31], the total difference in the lifetime of the clock state is about three times (see Table I).

The data on lifetimes for the states of both ions are presented in Table I. The present results are compared with experimental and other theoretical calculations. For the Yb III ion, Zhang *et al.* [32] have obtained the lifetime result for the $4f^{13}5d\ ^3P^o_1$ state both experimentally and theoretically. They performed the calculations using two variations of the RHF method of Cowan [45], which differ by the ways of inclusion of the CP effect.

B. Polarizabilities and blackbody radiation shifts

Static scalar polarizability $\alpha_v(0)$ of an atom in state v is given by

$$\alpha_v(0) = \frac{2}{3(2J_v+1)} \sum_n \frac{A^2_{vn}}{\omega_{vn}}, \tag{12}$$

where J_v is the total angular momentum of state v, A_{vn} are the amplitudes (reduced matrix elements) of the electric dipole transitions, ω_{vn} is the frequency of the transition. Equation (12) is valid when all wave-functions v and n are many-electron wave functions of the whole atom. It can also be used to calculate valence contributions to the polarizability if v and n are many-electron wave functions for the valence electrons only. Then, the contribution from core electrons

TABLE II. Transition amplitudes (A, a.u.) and transition probabilities (T, 1/s) evaluated with NIST frequencies for some low states of Cu II and Yb III ions. Semi. ≡ semiempirical.

		(ω), NIST [33]		Present		Other, T (s^{-1})		
Transition	Type	(cm^{-1})	(a.u.)	A (a.u.)	T (s^{-1})	Expt. [28]	Semi. [30]	Cal.
					Cu II			
$2 \leftrightarrow 1$	hfs-$E2$	21929	0.0999	$\sim 2 \times 10^{-4}$	$\sim 10^{-8}$[a]			
$3 \leftrightarrow 1$	$E2$	22847	0.1041	0.890	0.110			0.104, 0.157[b]
$3 \leftrightarrow 2$	$M1$	918	0.0042	$2.070\mu_B$	1.790×10^{-2}			1.70×10^{-2}[c]
$5 \leftrightarrow 1$	$E2$	26265	0.1197	−2.727	2.080			1.937, 2.687[b]
$7 \leftrightarrow 1$	$E1$	67917	0.3095	−0.182	$6.689 \times 10^{+6}$	$11.3 \times 10^{+6}$	$8.5 \times 10^{+6}$	$7.6 \times 10^{+6}$, $7.7 \times 10^{+6}$[d]
$7 \leftrightarrow 2$	$E3$	45988	0.2095	−0.346	5.459×10^{-8}			
$7 \leftrightarrow 3$	$E1$	45069	0.2054	2.489	$3.826 \times 10^{+8}$	$3.419 \times 10^{+8}$	$3.474 \times 10^{+8}$	$3.425 \times 10^{+8}$, $3.628 \times 10^{+8}$[d]
$7 \leftrightarrow 4$	$E1$	43918	0.2001	1.097	$6.875 \times 10^{+7}$	$6.29 \times 10^{+7}$	$6.35 \times 10^{+7}$	$6.29 \times 10^{+7}$, $7.16 \times 10^{+7}$[d]
$7 \leftrightarrow 5$	$E1$	41652	0.1898	0.379	$7.014 \times 10^{+6}$	$7.7 \times 10^{+6}$	$8.5 \times 10^{+6}$	$6.8 \times 10^{+6}$, $7.6 \times 10^{+6}$[d]
$7 \leftrightarrow 6$	$E2$	1498	0.0068	0.656	1.211×10^{-7}			
					Yb III			
$2 \leftrightarrow 1$	$M2$	33386	0.1521	$5.612\mu_B$	3.895×10^{-4}			1.662×10^{-4}[e]
$2 \leftrightarrow 1$	hfs-$E1$	33386	0.1521	$\sim 10^{-6}$	$\sim 10^{-4}$[a]			
$6 \leftrightarrow 1$	$E1$	39721	0.1810	0.308	$4.015 \times 10^{+6}$			$5.524 \times 10^{+6}$[e]
$6 \leftrightarrow 2$	$M1$	6335	0.0289	$1.583\mu_B$	5.726			5.702[e]
$6 \leftrightarrow 3$	$E2$	580	0.0026	0.909	2.017×10^{-9}			
$6 \leftrightarrow 5$	$E2$	4730	0.0216	7.202	4.579×10^{-3}			3.516×10^{-2}[e]
$7 \leftrightarrow 2$	$E2$	11891	0.0542	0.529	7.442×10^{-3}			5.209×10^{-3}[e]
$7 \leftrightarrow 6$	$M1$	5556	0.0253	$1.275\mu_B$	7.523			6.706[e]

[a] See Table III for details.
[b] Reference [29]; the first value was obtained using the Babushkin gauge, and the second value was obtained using the Coulomb gauge.
[c] Reference [46].
[d] Reference [30]; the first value was obtained using the length gauge, and the second value was obtained using the velocity gauge.
[e] Reference [31]; the value was obtained using the RMBPT method.

should be calculated separately. For the closed-shell core (or closed-shell atom or ion, such as Cu II or Yb III in the ground state), Eq. (12) can be reduced to

$$\alpha_v(0) = \frac{2}{3} \sum_c \langle v|\hat{d}|\delta\psi_c\rangle, \tag{13}$$

where $\hat{d}$ is the operator of the electric dipole moment and $\delta\psi_c$ is the RPA correction to the core state c [see Eq. (3)]. The summation goes over all states in the core. We neglect the change in the RPA corrections to the core states due to the excitation of an electron from the ground to the upper clock state. This is a small effect which is beyond the accuracy of our calculations.

TABLE III. Rates in s^{-1} for hfs-induced transitions from the clock states of Cu II and Yb III to the ground state.

Isotope	F	This paper	Reference [29]
^{63}Cu II	7/2	8.06×10^{-9}	9.19×10^{-9}
$I = 3/2,\ \mu = 2.2233$	5/2	7.64×10^{-9}	8.72×10^{-9}
	3/2	3.76×10^{-9}	4.29×10^{-9}
^{65}Cu II	7/2	9.25×10^{-9}	1.06×10^{-8}
$I = 3/2,\ \mu = 2.3817$	5/2	8.77×10^{-9}	1.00×10^{-8}
	3/2	4.32×10^{-9}	4.93×10^{-9}
^{171}Yb III	3/2	1.23×10^{-4}	
$I = 1/2,\ \mu = 0.4919$			
^{173}Yb III	7/2	8.41×10^{-5}	
$I = 5/2,\ \mu = -0.6776$	5/2	7.97×10^{-5}	
	3/2	3.92×10^{-5}	

To calculate the polarizabilities of the clock states, we use the approach developed in Ref. [47] for atoms or ions with open shells. It is based on Eq. (12) and the Dalgarno-Lewis method [48], which reduces the summation over the complete set of states to solving a matrix equation (see Ref. [47] for details). This approach treats the $3d$ electrons in Cu II and $4f$ electrons in Yb III as valence electrons. To calculate the contributions of the core electrons below the $3d$ or $4f$ shells, we use Eq. (13) in which the summation over the core state is limited to states below $3d$ or $4f$. To minimize the error in the difference between the ground state and the clock state polarizabilities, we use the same approach for both states of both ions.

The results are presented in Table IV. Our results for the ground-state polarizabilities are in excellent agreement with previous calculations. The polarizabilities of the excited states of Cu II and Yb III ions are calculated here.

The shift in the frequency of the clock transition due to blackbody radiation (BBR) is given by [51]

$$\delta\nu_{\rm BBR} = -1.6065 \times 10^{-6} \times T^4 \Delta\alpha(0), \tag{14}$$

where T is a temperature (e.g., room-temperature $T =$ 300 K), $\Delta\alpha(0) = \alpha_0(\text{c.s.}) - \alpha_0(\text{g.s.})$ is the difference between the clock state and the ground-state polarizabilities.

TABLE IV. Scalar static polarizabilities of the ground states α_0(g.s.s) and clock states α_0(c.s.s.) and BBR frequency shifts for the clock transition of ^{63}Cu II and ^{171}Yb III. $\delta\nu_{\rm BBR}/\omega$ is the fractional contribution of the BBR shift; where ω is the clock transition frequency.

	α_0(g.s.s) (a_B^3)		α_0(c.s.s.) (a_B^3)		BBR ($T = 300$ K)		
Transition	Present	Other cal.	Present paper	$\Delta\alpha(0)$	$\delta\nu_{\rm BBR}$ (Hz)	ω (Hz)	$\delta\nu_{\rm BBR}/\omega$
			Cu II				
$2 \leftrightarrow 1$	5.36	5.36[a]	24.12	18.76	−0.1616	$6.57 \times 10^{+14}$	-2.46×10^{-16}
$3 \leftrightarrow 1$	5.36	5.36[a]	24.05	18.69	−0.1610	$6.85 \times 10^{+14}$	-2.35×10^{-16}
			Yb III				
$2 \leftrightarrow 1$	6.39	6.55[b]	13.29	6.90	−0.0595	$1.00 \times 10^{+15}$	-5.95×10^{-17}

[a] Reference [49].
[b] Reference [50].

The calculated frequency shifts are presented in Table IV. The fractional BBR shifts for our Cu II are close in value to those of Zn: -2.5×10^{-16}, Cd: -2.8×10^{-16} [52], and Cu: -3.4×10^{-16} [26] and smaller than some other atomic clocks, such as Ca [53] and Sr [54] where the fractional BBR shift is at the level of 10^{-15}. As for the BBR shift in the Yb III clock transition, its fractional value of -5.95×10^{-17} is one of the smallest among optical clock transitions.

C. Zeeman shift and electric quadrupole shift

Clock transition frequencies might be affected by external magnetic and electric fields. Zeeman shift caused by magnetic field strongly depends on whether the atom or ion has a hyperfine structure. Both stable isotopes of copper (^{63}Cu and ^{65}Cu) have nonzero nuclear spin ($I = 3/2$) and nonzero hfs. On the other hand, five stable isotopes of Yb have zero nuclear spins and in two isotopes, spin is not zero (for ^{171}Yb $I = 1/2$ for ^{173}Yb $I = 5/2$). For atoms with zero nuclear spin, the first-order Zeeman shift can be avoided by considering transitions between states with $J_z = 0$, whereas the second-order Zeeman shift is small due to the absence of the hfs.

Below we consider isotopes with nonzero nuclear spin, ^{63}Cu and ^{171}Yb.

The linear Zeeman shift is given by

$$\Delta E_{F,F_z} = g_F \mu_B B F_z, \tag{15}$$

where g_F is the g factor of a particular hfs state. It is related to the electron g_J factor by

$$g_F = g_J \langle F, F_z = F, I, J|\hat{J}_z|F, F_z = F, I, J\rangle/F. \tag{16}$$

Electron g_J factors have values of $g_3 = 1.32$, $g_2 = 1.16$ for Cu II [33], and $g_2 = 1.46$ for Yb III (calculated value). The linear Zeeman shift can be suppressed by averaging over the transition frequencies with positive and negative F_z.

The second-order Zeeman shift for transition between definite hfs components is strongly dominated by transitions within the same hfs multiplet. Note that in this approximation, the shift is zero for the ground state (because $J = 0$). For the clock states, the shift is given by

$$\delta E_{F,F_z} = \sum_{F'=F\pm1,F'_z} \frac{|\langle F'F'_zIJ|\hat{J}_z|FF_zIJ\rangle x|^2}{\Delta E_{\rm hfs}(F,F')}, \tag{17}$$

where $x = g_J \mu_B B_m$ (in which g_J is electron g factors, μ_B is the electron magnetic moment, and B_m is a magnetic field), and $\Delta E_{\rm hfs}(F,F') = E(FIJ) - E(F'IJ)$ is the hfs interval. For more details, see Ref. [26].

To calculate this shift, we need to know the hfs of the clock states. We calculated the hfs using the CIPT and RPA methods as described above. The results for magnetic dipole hfs constants A and electric quadrupole hfs constants B are presented in Table V. Using these numbers and Eq. (17) we calculate the second-order Zeeman shift for all hfs components of the clock states of the ^{63}Cu II and ^{171}Yb III ions. The results are presented in Table VI. The shift is small and only slightly larger than in clock transitions of Cu, Ag, and Au [26]. As in the case considered in Ref. [26], the shift can be further suppressed by taking appropriate combinations of the transition frequencies. It might be even easier here since we need to worry only about suppressing the Zeeman shift for the clock state whereas it is already strongly suppressed for the ground state. The electric quadrupole shift is due to the interaction of the atomic quadrupole moment Q with the trapping the electric-field gradient and a corresponding term in the Hamiltonian is

$$H_Q = -\frac{1}{2}\hat{Q}_0 \frac{\partial \mathcal{E}_z}{\partial z}. \tag{18}$$

Here z is the quantization axis determined by the externally applied B field. The spherical components of the quadrupole moment operator $\hat{Q}_m = |e|r^2 C_m^{(2)}$ are the same as for the electric quadrupole ($E2$) transition. The energy shift of a state

TABLE V. Hyperfine structure constants A and B in (megahertz) of ^{63}Cu II and ^{171}Yb III ions. Nuclear spin I of (^{63}Cu) $= 3/2$ and I of (^{171}Yb) $= 1/2$, nuclear magnetic moment $\mu(^{63}\text{Cu}) = 2.2236(4)\mu_N$, and $\mu(^{171}\text{Yb}) = 0.49367(1)\mu_N$ [55]; nuclear electric quadrupole moment $Q(^{63}\text{Cu}) = -0.220(15)b$ [56] and $Q(^{171}\text{Yb}) = 0$.

No.	Conf.	Term	E (cm^{-1})	hfs A	hfs B
			^{63}Cu II		
1	$3d^9 4s$	$^3D_3$	21932	−186.46	−1.970
2	$3d^9 4s$	$^3D_2$	22733	−34.62	−1.097
			^{171}Yb III		
1	$4f^{13}5d$	$^3P^o_2$	29208	−41.46	0

TABLE VI. Second-order Zeeman shifts E_c [mHz/(μT)^2] for the clock states of ^{171}Yb III and ^{63}Cu II.

			$(\Delta E_c)/B_m^2$		
			^{63}Cu II		^{171}Yb III
No.	F_c	F_{cz}	$^3D_3$	$^3D_2$	$^3P_2^o$
1	1/2	±1/2		9.127	
2	3/2	±1/2	0.8687	−5.967	1.021
3	3/2	±3/2	0.5792	2.107	0.6807
4	5/2	±1/2	−0.3555	−2.265	−1.021
5	5/2	±3/2	−0.1515	−1.360	−0.6807
6	5/2	±5/2	0.2566	0.4478	0.000
7	7/2	±1/2	−0.3087	−0.8957	
8	7/2	±3/2	−0.2436	−0.7464	
9	7/2	±5/2	−0.1134	−0.4478	
10	7/2	±7/2	0.0818	0.000	
11	9/2	±1/2	−0.2045		
12	9/2	±3/2	−0.1841		
13	9/2	±5/2	−0.1432		
14	9/2	±7/2	−0.0818		
15	9/2	±9/2	0.000		

with total angular momentum J is proportional to the atomic quadrupole moment of this state. It is defined as twice the expectation value of the spherical component $Q_0 = Q_{zz}/2$ of the quadrupole operator in the stretched state,

$$Q_J = 2\langle J, J_z = J|\hat{Q}_0|J, J_z = J\rangle. \tag{19}$$

We calculate the values of Q_J using the CIPT and RPA methods. The results are $Q_3 = 0.537$ a.u. for the $^3D_3$ clock state of Cu II, $Q_2 = 0.299$ a.u. for the $^3D_2$ clock state of Cu II, $Q_2 = -2.369$ a.u. for the clock state of Yb III. Note that $Q = 0$ for the ground states of both ions because of the zero value of the total angular momentum J.

D. Sensitivity of the clock transitions to variation of the fine-structure constant

Dependence of frequencies of atomic transitions on the fine-structure constant in the vicinity of their physical values can be presented as

$$\omega = \omega_0 + q\left[\left(\frac{\alpha}{\alpha_0}\right)^2 - 1\right], \tag{20}$$

where α_0 and ω_0 are the present-day values of the fine-structure constant and the frequency of the transition and q are sensitivity coefficients that come from the calculations [15]. When one atomic frequency is measured against another over a long period of time, their relative time change is related to the time change of α by

$$\frac{\dot{\omega}_1}{\omega_1} - \frac{\dot{\omega}_2}{\omega_2} = (K_1 - K_2)\frac{\dot{\alpha}}{\alpha}. \tag{21}$$

The dimensionless value $K = 2q/\omega$ is usually called the *enhancement factor*. To calculate q (and K), we run computer codes at two different values of α and calculate the numerical derivative,

$$q = \frac{\omega(\delta) - \omega(-\delta)}{2\delta}, \tag{22}$$

where $\delta = (\alpha/\alpha_0)^2 - 1$ [see Eq. (20)]. The value of δ must be small to ensure linear behavior but sufficiently large to suppress numerical noise. Using $\delta = 0.01$ usually gives accurate results. The calculated values of q and K for clock transitions of Cu II and Yb III are presented in Table VII. As one can see, the sensitivity of the clock transitions of Cu II to variation of α is not very high, so they may be used as anchor lines for a comparison with a high-K transition [see Eq. (21)]. The sensitivity of the Yb III clock transition is one of the highest among the systems considered so far. It is close to the sensitivities of recently suggested clock transitions in Yb [22] and Au [26] and slightly smaller than the sensitivity of the most sensitive clock transitions in Yb II and Hg II [15].

IV. CONCLUSION

We have investigated a possibility to use Cu II and Yb III ions as optical ion clocks of high accuracy. Energy levels, lifetimes, transition rates, scalar static polarizabilities of the ground and clock states, and the BBR shifts have been calculated using the CIPT method. We have obtained a good agreement with previous data that are available to compare. Sensitivity to "new physics," such as variation of the fundamental constants has been studied. The uncertainty estimates

TABLE VII. Sensitivity of clock transitions to the variation of the fine-structure constant (q and $K = 2q/E$) for clock transitions in Cu II and Yb III.

No.	Conf.	Term	$E_{\text{exp.}}$ (cm^{-1})	q (cm^{-1})	K
			Cu II		
1	$3d^9 4s$	$^3D_3$	21929	−4350	−0.40
2	$3d^9 4s$	$^3D_2$	22847	−3700	−0.32
			Yb III		
1	$4f^{13} 5d$	$^3P_2^o$	33386	−42750	−2.56

for the Yb III ion and its high sensitivity to new physics indicate that Yb III atomic clock may successfully compete with the latest generation of clocks.

ACKNOWLEDGMENTS

This work was supported by the Australian Research Council Grants No. DP190100974 and No. DP200100150.

[1] Boulder Atomic Clock Optical Network [(BACON) Collaboration], Frequency ratio measurements at 18-digit accuracy using an optical clock network, Nature (London) **591**, 564 (2021).

[2] R. Lange, N. Huntemann, J. M. Rahm, C. Sanner, H. Shao, B. Lipphardt, C. Tamm, S. Weyers, and E. Peik, Improved Limits for Violations of Local Position Invariance from Atomic Clock Comparisons, Phys. Rev. Lett. **126**, 011102 (2021).

[3] C. Sanner, N. Huntemann, R. Lange, C. Tamm, E. Peik, M. S. Safronova, and S. G. Porsev, Optical clock comparison for Lorentz symmetry testing, Nature (London) **567**, 204 (2019).

[4] S. M. Brewer, J.-S. Chen, A. M. Hankin, E. R. Clements, C. W. Chou, D. J. Wineland, D. B. Hume, and D. R. Leibrandt, $^{27}Al^{+}$ Quantum-Logic Clock with a Systematic Uncertainty below 10^{-18}, Phys. Rev. Lett. **123**, 033201 (2019).

[5] T. Bothwell, D. Kedar, E. Oelker, J. M. Robinson, S. L. Bromley, W. L. Tew, J. Ye, and C. J. Kennedy, JILA SrI optical lattice clock with uncertainty of 2.0×10^{-18}, Metrologia **56**, 065004 (2019).

[6] N. Huntemann, C. Sanner, B. Lipphardt, C. Tamm, and E. Peik, Single-ion Atomic Clock with 3×10^{-18} Systematic Uncertainty, Phys. Rev. Lett. **116**, 063001 (2016).

[7] T. L. Nicholson, S. L. Campbell, R. B. Hutson, G. E. Marti, B. J. Bloom, R. L. McNally, W. Zhang, M. D. Barrett, M. S. Safronova, G. F. Strouse, W. L. Tew, and J. Ye, Systematic evaluation of an atomic clock at 2×10^{-18} total uncertainty, Nat. Commun. **6**, 6896 (2015).

[8] B. J. Bloom, T. L. Nicholson, J. R. Williams, S. L. Campbell, M. Bishof, X. Zhang, W. Zhang, S. L. Bromley, and J. Ye, An optical lattice clock with accuracy and stability at the 10^{-18} level, Nature (London) **506**, 71 (2014).

[9] K. Van Tilburg, N. Leefer, L. Bougas, and D. Budker, Search for Ultralight Scalar Dark Matter with Atomic Spectroscopy, Phys. Rev. Lett. **115**, 011802 (2015).

[10] Y. V. Stadnik and V. V. Flambaum, Can Dark Matter Induce Cosmological Evolution of the Fundamental Constants of Nature? Phys. Rev. Lett. **115**, 201301 (2015).

[11] Y. V. Stadnik and V. V. Flambaum, Improved limits on interactions of low-mass spin-0 dark matter from atomic clock spectroscopy, Phys. Rev. A **94**, 022111 (2016).

[12] A. Hees, J. Guena, M. Abgrall, S. Bize, and P. Wolf, Searching for an Oscillating Massive Scalar Field as a Dark Matter Candidate Using Atomic Hyperfine Frequency Comparisons, Phys. Rev. Lett. **117**, 061301 (2016)

[13] N. Leefer, A. Gerhardus, D. Budker, V. V. Flambaum, and Y. V. Stadnik, Search for the Effect of Massive Bodies on Atomic Spectra and Constraints on Yukawa-Type Interactions of Scalar Particles, Phys. Rev. Lett. **117**, 271601 (2016).

[14] A. D. Ludlow, W. F. McGrew, X. Zhang *et al.*, *Optical Frequency Measurements at* 1×10^{-18} *Uncertainty with Ytterbium Optical Lattice Clocks*, *Conference on Precision Electromagnetic Measurements (CPEM), Paris, France, JUL 08-13* (IEEE, Piscataway, NJ, 2018).

[15] V. V. Flambaum and V. A. Dzuba, Search for variation of the fundamental constants in atomic, molecular, and nuclear spectra, Can. J. Phys. **87**, 25 (2009).

[16] R. M. Godun, P. B. R. Nisbet-Jones, J. M. Jones, S. A. King, L. A. M. Johnson, H. S. Margolis, K. Szymaniec, S. N. Lea, K. Bongs, and P. Gill, Frequency Ratio of Two Optical Clock Transitions in $^{171}Yb^{+}$ and Constraints on the Time Variation of Fundamental Constants, Phys. Rev. Lett. **113**, 210801 (2014).

[17] V. A. Dzuba, V. V. Flambaum, M. S. Safronova, S. G. Porsev, T. Pruttivarasin, M. A. Hohensee, and H. Haffner, Strongly enhanced effects of Lorentz symmetry violation in entangled Yb^{+} ions, Nat. Phys. **12**, 465 (2016).

[18] J. C. Berengut, V. A. Dzuba, and V. V. Flambaum, Enhanced Laboratory Sensitivity to Variation of the Fine-Structure Constant Using Highly-Charged Ions, Phys. Rev. Lett. **105**, 120801 (2010).

[19] M. S. Safronova, V. A. Dzuba, V. V. Flambaum, U. I. Safronova, S. G. Porsev, and M. G. Kozlov, Highly Charged Ions for Atomic Clocks, Quantum Information, and Search for α variation, Phys. Rev. Lett. **113**, 030801 (2014).

[20] V. A. Dzuba and V. V. Flambaum, Highly charged ions for atomic clocks and search for variation of the fine structure constant, Hyperfine Interact. **236**, 79 (2015).

[21] M. S. Safronova, The Search for Variation of Fundamental Constants with Clocks, Ann. Phys. (Berlin) **531**, 1800364 (2019).

[22] V. A. Dzuba, V. V. Flambaum, and S. Schiller, Testing physics beyond the standard model through additional clock transitions in neutral ytterbium, Phys. Rev. A **98**, 022501 (2018).

[23] M. S. Safronova, S. G. Porsev, C. Sanner, and J. Ye, Two Clock Transitions in Neutral Yb for the Highest Sensitivity to Variations of the Fine-Structure Constant, Phys. Rev. Lett. **120**, 173001 (2018).

[24] S. G. Porsev, V. V. Flambaum, and J. R. Torgerson, Transition frequency shifts with fine-structure constant variation for Yb II, Phys. Rev. A **80**, 042503 (2009).

[25] V. A. Dzuba, V. V. Flambaum, and J. K. Webb, Calculations of the relativistic effects in many-electron atoms and space-time variation of fundamental constants, Phys. Rev. A **59**, 230 (1999).

[26] V. A. Dzuba, S. O. Allehabi, V. V. Flambaum, J. Li, and S. Schiller, Time keeping and searching for new physics using metastable states of Cu, Ag, and Au, Phys. Rev. A **103**, 022822 (2021).

[27] N. Kimura and M. Kajita, Prospect for precision measurement of the $Yb^{2+}\ ^1S_0 - {}^3P_0^o$ transition frequency, J. Phys. Soc. Jpn. **90**, 064302 (2021).

[28] E. H. Pinnington, G. Rieger, J. A. Kernahan, and E. Biemont, Beam-laser measurements and relativistic Hartree-Fock calculations of the lifetimes of the $3d^9 4p$ levels in Cu II, Can. J. Phys. **75**, 1 (1997).

[29] M. Andersson, K. Yao, R. Hutton, Y. Zou, C. Y. Chen, and T. Brage, Hyperfine-state-dependent lifetimes along the Ni-like isoelectronic sequence, Phys. Rev. A **77**, 042509 (2008).

[30] C. Z. Dong and S. Fritzsche, Relativistic, relaxation, and correlation effects in spectra of Cu II, Phys. Rev. A **72**, 012507 (2005).

[31] U. I. Safronova and M. S. Safronova, Correlation and relativistic effects for the 4f-nl multipole transitions in Yb III ions, Phys. Rev. A **79**, 032511 (2009).

[32] Z. G. Zhang, Z. S. Li, S. Svanberg, P. Palmeri, P. Quinet, and E. Biémont, Experimental and theoretical lifetimes in Yb III, Eur. Phys. J. D **15**, 301 (2001).

[33] A. Kramida, Yu. Ralchenko, J. Reader, and NIST ASD Team (2019). NIST Atomic Spectra Database (ver. 5.7.1), [Online]. Available: https://physics.nist.gov/asd [2020, September 26]. National Institute of Standards and Technology, Gaithersburg, MD.

[34] V. A. Dzuba, J. C. Berengut, C. Harabati, and V. V. Flambaum, Combining configuration interaction with perturbation theory for atoms with a large number of valence electrons, Phys. Rev. A **95**, 012503 (2017).

[35] W. R. Johnson and J. Sapirstein, Computation of Second-Order Many-Body Corrections in Relativistic Atomic Systems, Phys. Rev. Lett. **57**, 1126 (1986).

[36] W. R. Johnson, S. A. Blundell, and J. Sapirstein, Finite basis sets for the Dirac equation constructed from B splines, Phys. Rev. A **37**, 307 (1988).

[37] V. A. Dzuba, V. V. Flambaum, P. G. Silvestrov, and O. P. Sushkov, Correlation potential method for the calculation of energy levels, hyperfine structure and E1 transition amplitudes in atoms with one unpaired electron, J. Phys. B: At. Mol. Phys. **20**, 1399 (1987).

[38] W. R. Johnson, Hyperfine quenching: Review of experiment and theory, Can. J. Phys. **89**, 429 (2011).

[39] S. G. Porsev and A. Derevianko, Hyperfine quenching of the metastable $^3P_{0,2}$ states in divalent atoms, Phys. Rev. A **69**, 042506 (2004).

[40] V. A. Dzuba and V. V. Flambaum, Hyperfine-induced electric dipole contributions to the electric octupole and magnetic quadrupole atomic clock transitions, Phys. Rev. A **93**, 052517 (2016).

[41] B. G. C. Lackenby, V. A. Dzuba, and V. V. Flambaum, Calculation of atomic spectra and transition amplitudes for the superheavy element Db ($Z = 105$), Phys. Rev. A **98**, 022518 (2018).

[42] J. G. Li and V. Dzuba, Theoretical study of the spectroscopic properties of mendelevium ($Z = 101$), J. Quant. Spectrosc. Radiat. Trans. **247**, 106943 (2020).

[43] B. G. C. Lackenby, V. A. Dzuba, and V. V. Flambaum, Atomic structure calculations of superheavy noble element oganesson (Z=118), Phys. Rev. A **98**, 042512 (2018).

[44] B. G. C. Lackenby, V. A. Dzuba, and V. V. Flambaum, Theoretical study of the electron structure of superheavy elements with an open 6d shell: Sg, Bh, Hs, and Mt, Phys. Rev. A **99**, 042509 (2019).

[45] R. D. Cowan, *The Theory of Atomic Structure and Spectra* (University of California Press, Berkeley, CA, 1981).

[46] R. H. Garstang, Transition probabilities of forbidden lines, J. Res. Nat. Bur. Stand. A. Phys. Chem. **68A**, 61 (1964).

[47] V. Dzuba, Calculation of polarizabilities for atoms with open shells, Symmetry, **12**, 1950 (2020).

[48] A. Dalgarno and J. T. Lewis, The exact calculation of long-range forces between atoms by perturbation theory, Proc. R. Soc. London A **233**, 70 (1955).

[49] W. R. Johnson, D. Kolb, and K. Huang, Electric-dipole, quadrupole, and magnetic-dipole susceptibilities and shielding factors for closed-shell ions of the He, Ne, Ar, Ni (Cu^+), Kr, Pb, and Xe isoelectronic, At. Data Nucl. Data Tables **28**, 333 (1983).

[50] S. Harder, D. Naglav, P. Schwerdtfeger, I. Nowik, and R. H. Herber, Metal atom dynamics in superbulky metallocenes: A comparison of $(Cp^{BIG})_2Sn$ and $(Cp^{BIG})_2Eu$, Inorg. Chem. **53**, 2188 (2014).

[51] S. G. Porsev and A. Derevianko, Multipolar theory of blackbody radiation shift of atomic energy levels and its implications for optical lattice clocks, Phy. Rev. A **74**, 020502(R) (2006); **86**, 029904(E) (2012).

[52] V. A. Dzuba and A. Derevianko, Blackbody radiation shift for the $^1S_0$ - $^3P_0$ optical clock transition in zinc and cadmium atoms, J. Phys. B: At., Mol. Opt. Phys. **52**, 215005 (2019).

[53] G. Wilpers, C. W. Oates, S. A. Diddams *et al.*, Absolute frequency measurement of the neutral ^{40}Ca optical frequency standard at 657 nm based on microkelvin atoms, Metrologia **44**, 146 (2007).

[54] S. Blatt, A. D. Ludlow, G. K. Campbell, J. W. Thomsen, T. Zelevinsky, M. M. Boyd, J. Ye, X. Baillard, M. Fouché, R. Le Targat, A. Brusch, P. Lemonde, M. Takamoto, F.-L. Hong, H. Katori, and V. V. Flambaum, New Limits on Coupling of Fundamental Constants to Gravity Using ^{87}Sr Optical Lattice Clocks, Phys. Rev. Lett. **100**, 140801 (2008).

[55] N. J. Stone, Table of nuclear magnetic dipole and electric quadrupole moments, At. Data Nucl. Data Tables **90**, 75 (2005).

[56] N. J. Stone, Table of nuclear electric quadrupole moments, At. Data Nucl. Data Tables **111-112**, 1 (2016).